Composite Structures 381 (2026) 120006

Contents lists available at ScienceDirect

Composite Structures

journal homepage: www.elsevier.com/locate/compstruct

Influence of boehmite nanoparticles on moisture absorption and temperature effects in GFRP used for wind turbine blades☆

Maximilian Jux *, Thorsten Mahrholz, Peter Wierach

German Aerospace Center, Institute of Lightweight Systems, Lilienthalplatz 7, Braunschweig, Lower Saxony 38108, Germany

ARTICLE INFO

Keywords:
Nanoparticles
Moisture absorption
Temperature effects
Glass fiber reinforced composites (GFRP)
Boehmite
Tensile test

ABSTRACT

While boehmite nanoparticle integration enhances GFRP mechanical performance under standard conditions, their behavior under environmental stressors is less understood. This study investigates the effect of moisture absorption and temperature on nanoparticle-reinforced GFRP. A wind power-proven epoxy resin was modified with 5 and 10 wt% taurine-modified boehmite nanoparticles using a three-roll mill. Appropriate processing parameters are identified using viscosity and DSC measurements. Nanomodified GFRP composites are prepared via Vacuum Assisted Resin Infusion (VARI). Furthermore, the influence of moisture and temperature on GFRP properties, considering particle content and layer thickness, was investigated. Therefore, samples are stored under hot-wet conditions (50 °C; 70 % RH) until water saturation. Tensile properties of saturated and dry samples are then evaluated at test temperatures between − 20 °C and + 60 °C. Rheological tests have shown that the viscosity increases more quickly with rising temperature and increasing particle content. At the same time, the initial viscosity drops and the pot life extends by increasing the temperature, particularly for the particle-reinforced resins. DSC measurements confirm that the investigated particle modification only has a small impact on the epoxy system's cross-linking, while the addition of water leads to reduced cross-linking. Furthermore, the storage of GFRP samples under hot-wet conditions showed that particle modification leads to reduced moisture absorption, which, however, increases again with increasing particle content. Different mechanisms, particularly based on polarity and tortuosity effects, are discussed. The tensile tests reveal that storage under hot-wet conditions results in a decrease in secant modulus (up to 58 %), ultimate tensile strength (up to 53 %) and strain to failure (up to 62 %). This effect is more pronounced in materials with particle modification.

1. Introduction

The global share of wind power in energy generation is continuously expanding. Wind turbine power output is predominantly determined by rotor blade dimensions and wind speed. Given that wind conditions are uncontrollable, enlarging rotor blades remains the sole method to increase energy capture [1]. However, increasing the size proportionally elevates mechanical loads and material requirements. Furthermore, wind turbines are often subjected to rough climatic conditions and substantial loads from high wind speeds. Operating temperatures typically range from − 20 °C to + 50 °C [2], causing both reversible and irreversible changes in the polymer matrix. Depending on the installation site, significant stresses such as erosion from rain, snow, or ice are common, too. Higher temperatures and humidity in tropical and subtropical climates can also impose severe material challenges.

All these environmental factors can significantly degrade the thermal and mechanical properties of fiber-reinforced plastics (FRPs) [2–6], especially the matrix dominated properties [2]. As rotor blade dimensions and environmental stresses intensify, conventional materials are reaching their operational limits. Consequently, there is substantial demand for innovative materials offering enhanced performance. The development of nanomodified material systems might present a key strategy to address this growing material need. Nanoparticles possess significant potential due to their inherent properties. Paschen et al. [7] demonstrated that nanoparticles can alter nearly all chemical and physical properties of polymers, reporting up to 80 % increase in mechanical properties with just 5 wt% filler content.

But nanoparticles can also lead to increased water uptake, especially

☆ This article is part of a special issue entitled: 'Rolfes 65th' published in Composite Structures.

* Corresponding author.
E-mail addresses: maximilian.jux@dlr.de (M. Jux), thorsten.mahrholz@dlr.de (T. Mahrholz), peter.wierach@dlr.de (P. Wierach).

https://doi.org/10.1016/j.compstruct.2025.120006
Received 31 July 2025; Received in revised form 19 December 2025; Accepted 22 December 2025
Available online 23 December 2025

if they possess hydrophilic surfaces that can form strong hydrogen bonds [8]. Liu et al. [9] reported that hydrophilic particles increased both water absorption and diffusion rates. Additionally, they found that hydrophobic particles have the opposite effect. These effects have also been observed in similar studies [10,11]. Nomai [12] identifies two primary effects of nanoparticles influencing the water uptake. They can act as impermeable barriers, creating a tortuosity effect, or they can increase the free volume (e.g., interphases, interstices of agglomerates). Gatos et al. [13] also investigated the water absorption depending on particle size. They found that water absorption decreased with increasing particle size (lower specific surface area). Water molecules can also interact with the polar groups of resin and hardener molecules [14]. This interaction can significantly influence the network structure and mechanical properties of the resin system. Soles et al. [15] attribute to water the ability to modify the topology of resin systems, specifically by exposing additional polar bonding points. The incorporation of water molecules can also cause a softening of the matrix caused by chain separation, a process widely referred to as plasticization [2,6,14,16–18]. Furthermore, water absorption leads to matrix swelling. This process expands the free volume within the matrix, resulting in increased water absorption and a rise in internal stress [4,19]. Several studies [6,14,16,17] also report, that swelling stresses within the matrix and water inclusions can cause the formation of cracks and a reduction of interfacial strength between fiber and matrix leading to a debonding of the fibers. A risk that escalates with the material's maximum water absorption.

Temperature also influences the properties of FRPs significantly, as outlined by Jayaram [4,20]. These impacts vary depending on the temperature range. Cryogenic temperatures lead to embrittlement and reduced shear strength. Absorbed moisture can also expand and produce internal stresses and damage. Different thermal expansion behaviour of matrix and fiber may induce stress cracks, too. Prolonged exposure to higher temperatures can trigger material aging, diminishing strength properties. Exceeding the glass transition temperature (Tg) results in material softening. Once the decomposition temperature is reached, the FRP can be irreversibly destroyed. Beyond these static influences, alternating thermal stresses can also induce microcracks reducing mechanical strength [4]. Li [2] further demonstrates a clear temperature dependency in glass fiber-reinforced resin systems, primarily affecting matrix-dominated properties. These can occur in both dry and wet conditions, with water absorption intensifying the effects.

Building upon previous work, this study investigates the impact of moisture and temperature on glass fiber-reinforced polymer (GFRP) composites modified with nanoparticles, particularly focusing on boehmite. Boehmite nanoparticles are of interest due to their low cost, commercial availability, and proven ability to significantly enhance the mechanical properties of epoxy resin systems and the matrix-dominated mechanical properties of fiber-reinforced composites under standard conditions [21]. Previous research has identified particle size and filler content as primary factors influencing mechanical performance [21–23]. Furthermore, while surface modification (e.g., with taurine) of boehmite nanoparticles does not significantly affect mechanical properties, it substantially improves resin processability [21,24]. The enhanced static and fatigue mechanical properties achieved with boehmite nanoparticles have been successfully transferred to GFRP, a composite widely used in the wind power industry [25]. This study extends the preliminary work by examining the effects of moisture and temperature on the thermal, rheological and mechanical properties of boehmite nanoparticle-modified epoxy resins and corresponding GFRP, utilizing water absorption tests as wells as DSC, rheometer and tensile measurements.

2. Materials

For the preparation of particle-modified and unfilled resin test samples, as well as corresponding GFRP test plates, Epikote RIMR 035c epoxy resin and Epikure RIMH 038 amine hardener were used as the polymer matrix. Hexion supplied both components, which are approved by Germanischer Lloyd (DNV GL) for wind turbine blade manufacturing. The epoxy resin is a mixture of epoxy oligomers: bisphenol-A-diglycidyl-ether resin, bisphenol-F-diglycidyl-ether resin and alkyl-(C12-C14)-glycidyl ether derivatives acting as a reactive solvent. Both the bisphenol-F and the reactive solvent lower the viscosity and reduce the tendency of crystallization [21]. The hardener is composed of linear and cyclic diamines: 1,2-ethanediol di(oxybutylene) diamine and 3-aminomethyl-3,5,5-trimethylcyclohexylamine. The mixing ratio of resin to hardener was 100:28 by weight. Mixing was performed at room temperature, followed by a brief degassing step. The curing cycle was set at 80 °C for 5 h. This resin system exhibits low vapor pressure, enabling curing under vacuum, which is beneficial for VARI and RTM processes. The fully crosslinked resin system, without additional additives, has a glass transition temperature (Tg) of approximately 80 °C. It is important to note that small quantities of moisture can accelerate the curing reaction and influence the mechanical properties.

A unidirectional E-glass fabric (Saertex U-E-1182 g/m^2–1270 mm), commonly used in the wind power industry, served as the fiber semi-fabric for GFRP test plate manufacturing. This fabric features a single layer of unidirectional E-glass fibers (0°, 2400 TEX, 1134 g/m^2) and perpendicular weft yarns (90°, E-glass 68 TEX, 36 g/m^2). The fabric is sewn with PES (76 dtex, 12 g/m^2) in a tricot-warp seam pattern.

Boehmite nanoparticles with taurine surface modification (Disperal HP 14/taurine from Sasol, abbreviated HP14T) were incorporated as a filler into the epoxy resin system and corresponding GFRP plates. According to the manufacturer's specifications, these particles exhibit a specific surface area of 184 m2/g, a bulk density of 0.41 g/ml, an average agglomerate particle size (D50 value) of 17 μm and an average primary particle size of 14 nm. Boehmite, a γ-aluminum hydroxide with the chemical formula AlO(OH), possesses reactive hydroxyl groups on its surface, making them suitable for bonding surface modifications. The interactions between the resin system and the nanofiller are crucial for achieving property improvements, primarily due to the resulting interphase. This interphase, characterized by a differing network density, exhibits properties distinct from the bulk resin. Both particle size and surface modification govern the interphase structure and the resulting mechanical properties. The taurine (2-aminoethanesulfonic acid) used as a surface modifier here attaches to the particle surface through an electrostatic interaction (outer sphere complex) between a reactive hydroxyl group on the particle and an oxygen atom of its sulfonate group as illustrated in Fig. 1 [24]. The following abbreviations are used for material designations throughout the paper: “Ref” refers to the resin and fiber composite without particles, “05HP14T” to resin and fiber composite with 5 wt% taurine-modified boehmite nanoparticles and “10HP14T” to resin and fiber composite with 10 wt% taurine-modified boehmite nanoparticles.

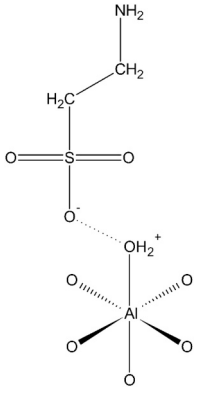

Fig. 1. Illustration of outer-sphere complex between taurine and boehmite nanoparticle surface.

3. Methods

3.1. Resin preparation

For the preparation of a masterbatch, HP14T particles were mixed into the epoxy resin component with a weight fraction of 20 wt%. The dispersing process was realized with a three-roll mill (EXAKT 80 E) to ensure homogeneous particle distribution and comminution of the agglomerates. The three-roll mill consists of three counter-rotating, coaxial rollers with a speed ratio of 9:3:1 (Fig. 2). The particles are crushed by means of shear forces and expansion flows, triggered by different rotation speeds of the rollers. The load increases until shortly before the minimum gap size is reached. This is followed by a sudden release in the form of a drop in pressure, which favors particle wetting. The level of the shear forces that occur is influenced by various factors. Viscosity plays a major role. High viscosities lead to greater shear stresses and thus to an increased dispersing effect. Therefore, high particle concentrations, low process temperatures and high particle–matrix interactions have a positive effect on the dispersion process. Other influencing factors are the gap sizes. Smaller gaps lead to higher stresses. The rotational speeds of the rollers also have an influence on the dispersion process. High peripheral speeds can briefly increase the fluid speed and therefore the shear stress. However, they also lead to increased temperatures and thus to a reduction in resin viscosity. In addition to affecting viscosity, temperature also plays an important role in controlling possible reactions between resin and particles. Higher temperatures result in faster reaction processes.

For this reason, additional cooling (20 °C) of the rollers during the dispersion process was implemented. A characteristic feature of the dispersion of boehmite particles in epoxy resin is that the transparency of the dispersion increases as the dispersion process progresses. This indicates a decreasing particle/agglomerate size and a more homogeneous distribution. The dispersed masterbatch is stored at freezing temperatures (−20 °C) to counteract re-agglomeration and sedimentation processes. The gap stresses can be affected by changing either the gap size or the contact force between the rollers. In general, the throughput decreases with smaller gap sizes and higher gap stresses. The process parameters for dispersing the HP14T particles in the resin component RIMR 035c are listed in Table 1.

In the next step, the masterbatch is diluted with resin and hardener to achieve the desired target nanoparticle concentration of 5–10 wt%. It has to be ensured that for each concentration the resin to hardener ratio is 100 to 28 wt%. The components are added to a mixing container starting with the masterbatch. The quantities are weighed with an accuracy of 0.01 g. A double asymmetric centrifugal mixer (Hausschild "SpeedMixer DAC 700.2 VAC-P") is used for the mixing process, see Fig. 3. This mixer rotates in two opposite directions, with the disc rotating at approximately four times the speed of the sample container. To eliminate entrapped air, the mixing container is kept under vacuum. Table 2 details the specific process parameters for the identified mixing steps for getting the best dispersion qualities.

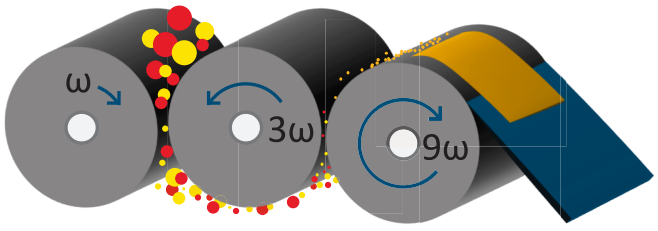

Fig. 2. Functional principle of a three-roll mill.

Table 1
Process parameter for dispersing process with three-roll mill.

Mode	Gap size/contact force		Repetitions	Rotational speeds (back: middle:front)
	Rear gap	Front gap		
Gap mode	150 µm	50 µm	3	150:50:16.67 1/min
	45 µm	15 µm	5	
	15 µm	5 µm	5	
Force mode	15 N/mm	15 N/mm	2	

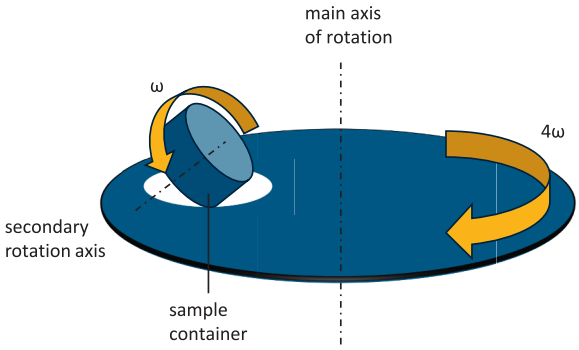

Fig. 3. Functional principle of a double asymmetric centrifugal mixer.

Table 2
Process parameter for mixing with centrifugal mixer.

Section	Time(s)	Speed(1/min)	Air pressure(mbar)
1	150	0	3
2	50	1500	3
3	50	1900	3

3.2. Dispersion quality

The particle size distribution of the prepared HP14T nanoparticle masterbatch in epoxy resin was analyzed using a disc centrifuge (DC24000; CPS Instruments), which permits particle size determination from 5 nm to 50 µm. The analyzer determines the particle size distribution via centrifugal sedimentation within an optically clear spinning disc filled with a fluid. The fluid is based on a density gradient to stabilize sedimentation. A series of different mixtures of epoxy resin and MEK were used to create this gradient. The particle size distribution was determined based on three measurements. Fig. 4 depicts the cumulative distribution curve (Q3) and the distribution density curve (q3) of an exemplified measurement. The resulting narrow particle distribution with a mean x50 value of 110 nm confirms the homogeneous nanoparticle dispersion with minimal agglomeration. This finding is further supported by a SEM image (Fig. 5) of the cured nanocomposite (10 wt% HP14T). Both the CPS and SEM analyzes reveal that the calendering process results in good nanoparticle dispersions. Nevertheless, this way the manufacturer's specified primary particle size of 14 nm could not be recreated.

3.3. Production of test plates

Composite test plates were manufactured using an adapted Vacuum-Assisted Resin Infusion (VARI) process. This modification facilitates rapid through-thickness infusion, which is essential for processing high-viscosity resins. The setup is schematically shown in Fig. 6. All surfaces that come into contact with resin during the production process (base plate and pressure plate) were treated with a water-based release agent.

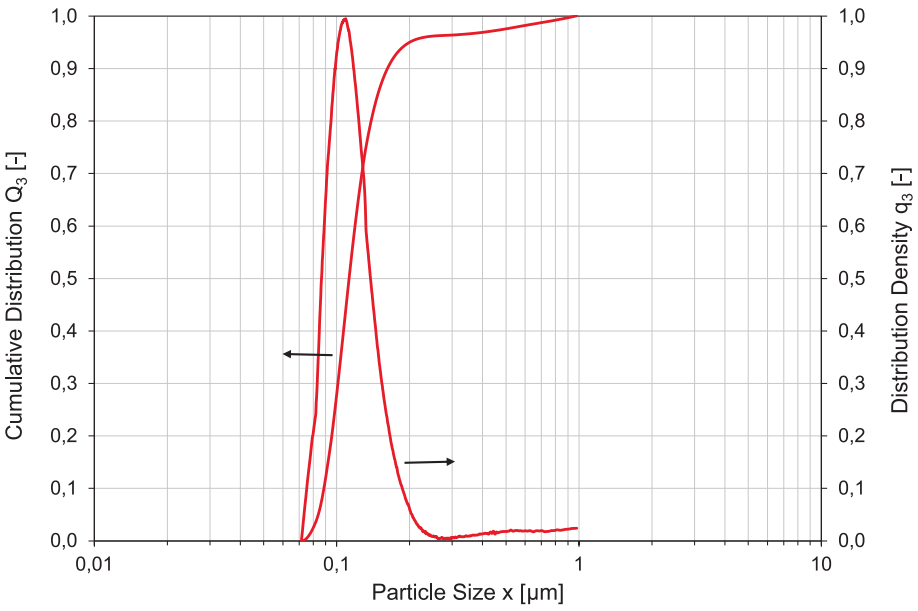

Fig. 4. Normalized distribution curves Q3 and q3 of the master batch with 20 wt% HP14T in epoxy resin, determined using a disc centrifuge.

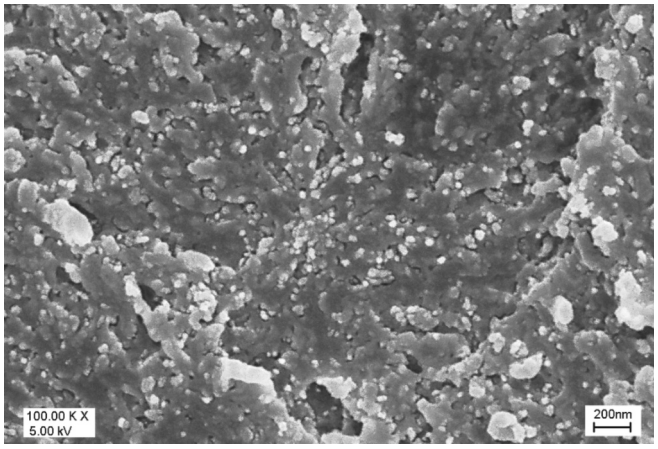

Fig. 5. SEM image of a nanocomposite with 10 wt% HP14T in epoxy resin. Surface generated by cryoscopic fracture.

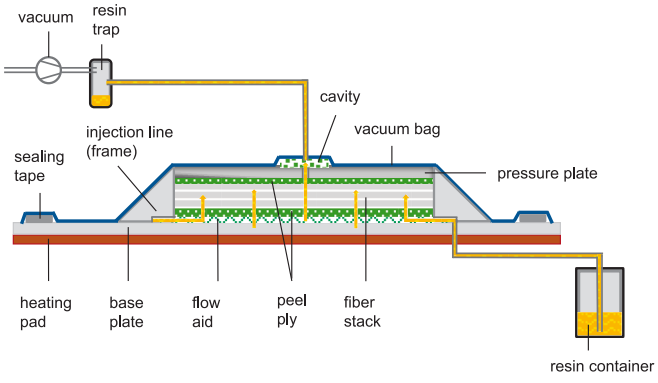

Fig. 6. Schema of the infusion process.

A layer of flow aid was first placed on the base plate to ensure that the structure is impregnated throughout the thickness of the layup. A layer of peel ply was then placed on the flow aid. This simplifies the demolding process. On top of the peel ply unidirectional glass fiber layers are stacked. The samples for determining the water absorption were manufactured with 1 to 3 and the tensile samples with 2 unidirectional fiber layers. Following this, another layer of peel ply was placed above the glass fiber layers so that both surfaces of the test plate have the same structure. Next, a pressure plate was placed on the final layup to create a constant overall thickness. A central hole in the pressure plate allowed the connection of a vacuum line. Before vacuum bagging, the entire setup was enclosed in a metal frame, enabling the resin system to flow into the layup simultaneously from all sides (circular infusion line and a separate vacuum line). To improve infusibility, the evacuated setup was maintained at 40 °C using a heating pad. The infusion process continued until the structure was fully impregnated. The infusion time varied from a few minutes to over 30 min, depending on the resin system's viscosity, the number of fiber layers and the plate's size. To maintain the low viscosity of the thixotropic resin system, it was continuously stirred throughout the entire infusion time. Once the infusion was complete, the layup was cured in an oven for 5 h at 80 °C. After demolding, the quality of the test plates (absence of dry spots and pores) was confirmed using ultrasonic scans. All GFRP test plates manufactured show an FVC of 53–55 %, a typical value for composites manufactured by VARI process. GFRP specimens were prepared by cutting with a circular saw using a diamond saw blade. The specimens did not receive additional surface treatment after cutting.

3.4. Determination of the pot life

The pot life, defining the maximum processing time of resin, was determined by measuring the viscosity with a rheometer (MCR 702 MultiDriveTM, Anton Paar). Every material combination and test condition was characterized with 3 specimen. For the infusion process in FRP production, resin systems should not exceed a viscosity limit value of 0.5 Pas. Higher viscosities, especially in nanomodified resin systems, lead to longer infusion times as the flow rate decreases. Since both crosslinking speed and pot life are temperature-dependent, the resin systems are analyzed at various temperatures. Measurements were performed using a plate-plate arrangement with a 25 mm diameter and a 1 mm measuring gap. All measurements were carried out isothermally and at a constant shear rate of 40 1/s.

3.5. Determination of enthalpy and glass transition temperature

The specific reaction enthalpies and glass transition temperatures of the pure and nanoparticle-modified resins were determined using dynamic differential calometry (DSC822e, Mettler Toledo). For every material combination 3 samples were tested. During the measurement, the physical or chemical transformation of a resin system is determined on the basis of the heat flow. The mass of the sample was determined with an accuracy of 0.01 mg. The enthalpy measurement is realized isothermally at 80 °C for a duration of 300 min. This corresponds to the recommended curing parameters and ensures complete curing. In addition to the influence of the nanoparticles, the influence of water on the reaction enthalpy was also investigated. For this purpose, water with a weight proportion of 1 % was added to the samples using the centrifugal mixer. This proportion of water is considered realistic based on the results of the saturation tests. To determine the glass transition temperatures, the cured material systems were heated from 20 °C to 160 °C at a heating rate of 10 $K \cdot min^{-1}$. During the glass transition, a material-specific step increase in the specific heat capacity of the resin system is observed. This step is used to determine the glass transition temperature in the DSC measurements.

3.6. Determination of moisture absorption

To investigate the diffusion behavior and maximum water absorption of GFRP, samples were stored under hot-wet conditions and weighed at defined intervals until saturation (with an accuracy of 0.1 mg). This study analysed the influence of material thickness and nanoparticle content on these properties. Before storage, samples as depicted in Fig. 7 were dried for 28 days at 50 °C and 10 % relative humidity (RH). After three days, the temperature was increased to 70 °C. This drying process aimed to remove any existing moisture, enabling the recording of the entire saturation process. Once the samples reached a constant mass, they were transferred to a climate chamber and stored under defined hot-wet conditions (50 °C, 70 % RH). The saturation curves are determined according to DIN EN 2823 using four square samples each with a side length of 50 mm, which means that the thicknesses are significantly smaller than the sample lengths and widths.

3.7. Tensile tests

According to DNVGL-ST-0376 relevant loads for rotor blade design are bending and torsional moments, axial and shear forces, as well as fatigue loads. Furthermore, and especially for specific requirements like higher and lower temperatures the following tests shall be included in material testing: laminate compression strength in fiber direction, laminate tensile static strength perpendicular to fiber direction, laminate in-plane shear static strength testing. Since, this work aims to modify the laminates matrix to improve the overall rotor blade properties, a simple test that is dominated by the matrix properties was chosen (static tensile test perpendicular to fiber direction). The tensile properties are determined on unidirectional specimens perpendicular to the fiber direction based on DIN EN 2597. Specifically, the width and length of the samples are according to the standard, however, specimens were tested without tabs, because of concerns about potential effects on the moisture uptake during specimen conditioning. Further, the number of samples tested for each test condition and material type (summarized in Table 3), however, is lower than the required minimum of at least ten. The Zwick 1484 electromechanical universal axial testing machine is used for the tests. Fig. 8 shows the test setup. The tests are caried out at − 20 °C, 23 °C and 60 °C. The temperatures of − 20 °C and 60 °C are assumed to be the maximum operating temperatures of the resin system. The influence of water absorption at different test temperatures on the mechanical properties of the tested material systems is therefore to be determined. In addition, the influence of the HP14T nanoparticles on these effects will be investigated. The tensile test procedure can be roughly divided into the following steps. All samples are stored in a climate chamber at higher temperatures and humidity until saturation. Before testing the saturated samples were cooled down to room temperature. To do this, all samples of one series are removed from the climate chamber and placed in an airtight container. In this container, the samples can be cooled down to room temperature without absorbing moisture during the cooling process. The samples are only removed from the airtight container for testing immediately before the test start. The aim is to create the same initial conditions between the stored and non-stored samples. In the next step, the samples are suspended in the clamping device and heated or cooled to test temperature in the temperature chamber for approximately 5 min. The tests are performed at a constant testing speed of 1 mm/min until failure occurs. During this process, the tensile force, strain and time were recorded. Force was measured using a 20 kN force transducer. Strain was captured using an MTS 632.85F-14 biaxial extensometer, which has a measuring length of 25 ± 0.05 mm and a temperature range of − 100 °C to + 150 °C. Conical tips ensured contact between the extensometer and the sample. The extensometer was applied after reaching a 5 N preload. A constant test speed of 1 mm/min was maintained.

Fig. 7. Samples stored under hot-wet conditions. Left: Samples for determining the saturation curve. Right: 90° tensile samples.

4. Results and discussion

4.1. Rheological tests

Resin systems suitable for the VARI process should have the longest possible pot life and low initial viscosity. Fig. 9 shows the rheological behavior of the epoxy system under investigation as a function of filler content and temperature (23 °C, 40 °C, 50 °C). In the diagram, the viscosities up to 100 Pas are considered over a maximum period of 600 min. Observation over a longer period of time and a broader viscosity range allows statements to be made about viscosity build up. During the curing process, the resin reacts with the hardener, resulting in cross-linking at a molecular level. The viscosity therefore increases with increasing cross-linking, as the molecules are increasingly restricted in their movement.

The results show that an increase in temperature leads to a significantly accelerated viscosity build up. While viscosities of up to 35 Pas

Table 3
Number of samples tested for each material system and test condition.

Matrix type	Test temperature (°C)	Number of dry samples	Number of saturated samples
Ref	-20	5	5
	23	4	5
	60	5	5
05HP14T	-20	5	5
	23	5	5
	60	5	5
10HP14T	-20	5	5
	23	4	5
	60	5	5

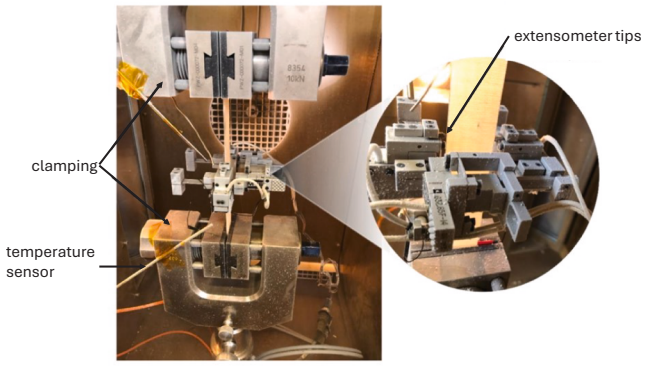

Fig. 8. Tensile test setup (left), applied biaxial extensometer (detailed view on the right).

are achieved after 600 min at room temperature, an increase in temperature to 40 °C leads to viscosities exceeding 100 Pas after only approximately 300 min. By further increasing the temperature to 50 °C, a viscosity of 100 Pas is reached after approximately 190 min. Modifying the epoxy system with HP14T nanoparticles leads to an additional increase in the curing speed. The effect is small at a particle content of 5 wt%. The viscosity values at around 45 Pas after 600 min at 23 °C are only slightly higher than the values measured for the epoxy system without particles. Even at 40 °C, a viscosity of 100 Pas is only reached around 22 min earlier. At a particle content of 10 wt%, the effects are more pronounced. At a test temperature of 23 °C, this resin system already reaches a viscosity of approximately 100 Pas after 600 min. At 40 °C, the time to exceed 100 Pas decreases by around 60 min, and at 50 °C it decreases by around 44 min compared to the unmodified epoxy system. Fillers increase the viscosity as they increase the internal friction of the resin system. The extent to which the viscosity is increased depends on the particle size (specific surface area) and the filler content. In addition, it cannot be ruled out that the HP14T nanoparticles might have a catalytic effect and therefore contribute to the accelerated viscosity build up [26,27].

Fig. 10 (enlarged area of Fig. 6) shows the viscosity curves of the epoxy systems up to a maximum of 2 Pas and 200 min. This clearly shows the initial viscosities and pot lives of the epoxy systems analyzed. The initial viscosities correspond to the points of contact of the

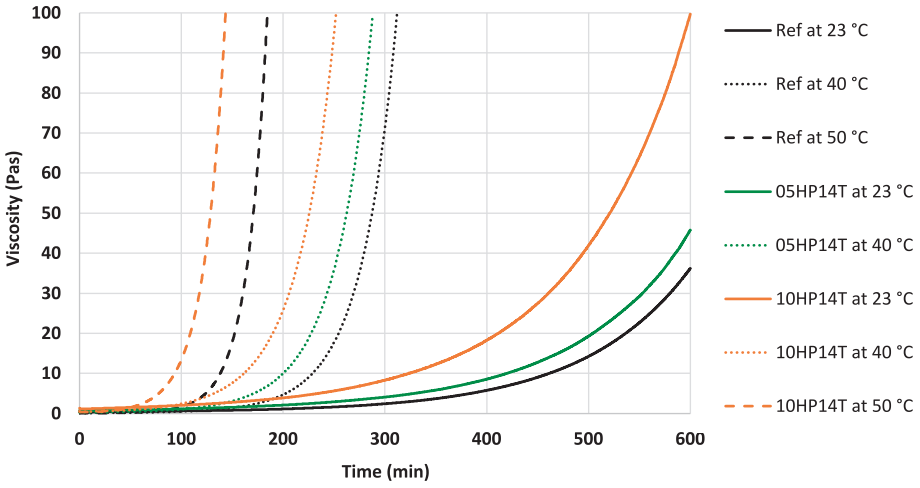

Fig. 9. Averge dynamic viscosity curves of epoxy–HP14T nanocomposites as function of process time, temperature and particle content. Conditions: Isothermal measurement with constant shear rate (40 1/s) and gap size (1 mm) using plate-plate arrangement with a plate diameter of 25 mm. Content of HP14T nanoparticles: 5 and 10 wt%; epoxy resin: EPIKOTE RIMR 035c / EPIKURE RIMH 038.

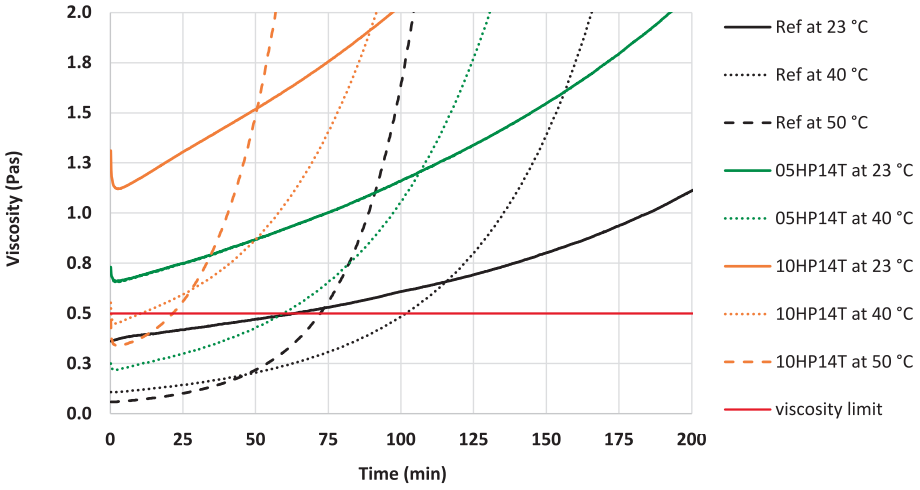

Fig. 10. Average initial viscosities and pot life of epoxy–boehmite nanocomposites as function of process time, temperature and particle contents. Conditions: Isothermal measurement with constant shear rate (40 1/s) and gap size (1 mm) using plate-plate arrangement with a plate diameter of 25 mm. Content of HP14T nanoparticles: 5 and 10 wt%; epoxy resin: EPIKOTE RIMR 035c / EPIKURE RIMH 038.

measurement curves with the Y-axis. Due to the epoxy systems being processed in an infusion process, the empirical viscosity limit value is set to 0.5 Pas. The pot lives of the epoxy systems correspond to the intersections of the measurement curves with the viscosity limit. The initial viscosity of the unmodified epoxy system is below the viscosity limit value of 0.5 Pas at all temperatures analyzed. It can also be seen that an increase in temperature leads to a reduction in the initial viscosity. At a temperature change from 23 °C to 40 °C, this drop in viscosity is just under 0.25 Pas and leads to an increase in pot life of around 50 %. A further increase in temperature to 50 °C only leads to a slight reduction in viscosity of 0.05 Pas, but due to the accelerated viscosity build up, the pot life measured is almost the same compared to a temperature of 23 °C.

In the case of nanoparticle-filled epoxy systems, an increase in temperature also leads to a reduced initial viscosity. In addition, a strong decrease in viscosity can be detected at the very beginning of the measurement for the modified epoxy systems. This effect highlights the thixotropic properties of the nanoparticle-modified resin system attributed to particle–particle and particle–matrix interaction. Initially, intensive particle–particle interactions control the viscosity. Applied shear stress disrupts or destroys these pre-structures, leading to a decrease in the observed viscosity. Additionally, bonds between particles and the resin matrix can break under shear stress, further contributing to the reduction of viscosity. The short molecular chain of the taurine surface modification, comprising two CH2 groups and an amino group, extends into the resin system serving as a binding partner. Given the high reactivity of amino groups, a bond between the nanoparticles and the resin system is anticipated. As a result, at a temperature of 23 °C, the viscosity limit (0.5 Pas) cannot be undercut at a particle content of either 5 wt% or 10 wt%. At a temperature of 40 °C, the viscosity falls below the viscosity limit due to the reduced initial viscosity at a particle content of 5 wt%, whereby a pot life of approximately 60 min can be achieved. However, at a particle content of 10 wt%, the significant increase in initial viscosity drastically reduces the pot life. Consequently, the temperature must be raised to 50 °C to keep the viscosity below the specified limit. This elevated temperature, however, accelerates viscosity build up, resulting in pot lives of just over 20 min. Based on these results, the viscosity of particle-modified epoxy systems can be reduced by both increasing temperature and applying shear stress. During the infusion process, for instance, shear stress can be achieved by stirring the epoxy system. This way, the range of essential processing parameters for the fabrication of nanoparticle-modified GFRP laminates has been successfully identified.

4.2. DSC tests

Differential Scanning Calorimetry (DSC) measurements were conducted to assess how boehmite nanoparticles and water influence the curing behavior of the epoxy resin used. Nanoparticle content was varied from 5 to 10 wt%, corresponding to concentrations used in the rheological measurements. Recognizing the inherent hygroscopic properties of the epoxy resin, particularly its amine hardener, which could potentially impact the curing process, a water content of 1 wt% was determined to be appropriate for these studies.

The curves recorded during the isothermal DSC measurement correspond to the time dependent weight-related heat flows. The curves show a clear peak, which results from the exothermic cross-linking of the resin system and the areas under the measured curves indicate the enthalpy released during the reaction. The specific enthalpies determined can also be referred to as total reaction enthalpies and are shown on the left-hand side of Fig. 11. By comparing the total enthalpy of reaction, the extent of chemical bond formation between the individual material systems can be assessed. The enthalpy values in J/g drop with increasing particle content and due to the addition of 1 wt% water. The enthalpy of the unmodified reference is 426 J/g. The addition of 5 wt% HP14T nanoparticles leads to a drop of approximately 7.2 %. At a particle content of 10 wt%, the reaction enthalpy decreased by 10.9 %. This reduction is attributed to the substitution of the reactive resin by the particle mass. Although some chemical bonding at the interface with the resin system is possible, the HP14T nanoparticles themselves do not significantly contribute to the total exothermic enthalpy. The measured enthalpy was normalized to account for the reduced proportion of reactive resin and hardener components due to particle loading. The normalized enthalpies show only slightly lower values than the reference system. In a preliminary study, a slight reduction in the reaction enthalpy was also observed with an increasing content of HP14T nanoparticles in an epoxy resin [24]. The effect was explained by a steric hindrance in the cross-linking of resin and hardener molecules by the particles. The samples with a water content of 1 wt% undergo a reduced cross-linking process. The decrease in enthalpy is around 3.6 % for the unmodified reference and around 5.3 % for the resin system with 10 wt % HP14T nanoparticles. The observed decrease in the measured

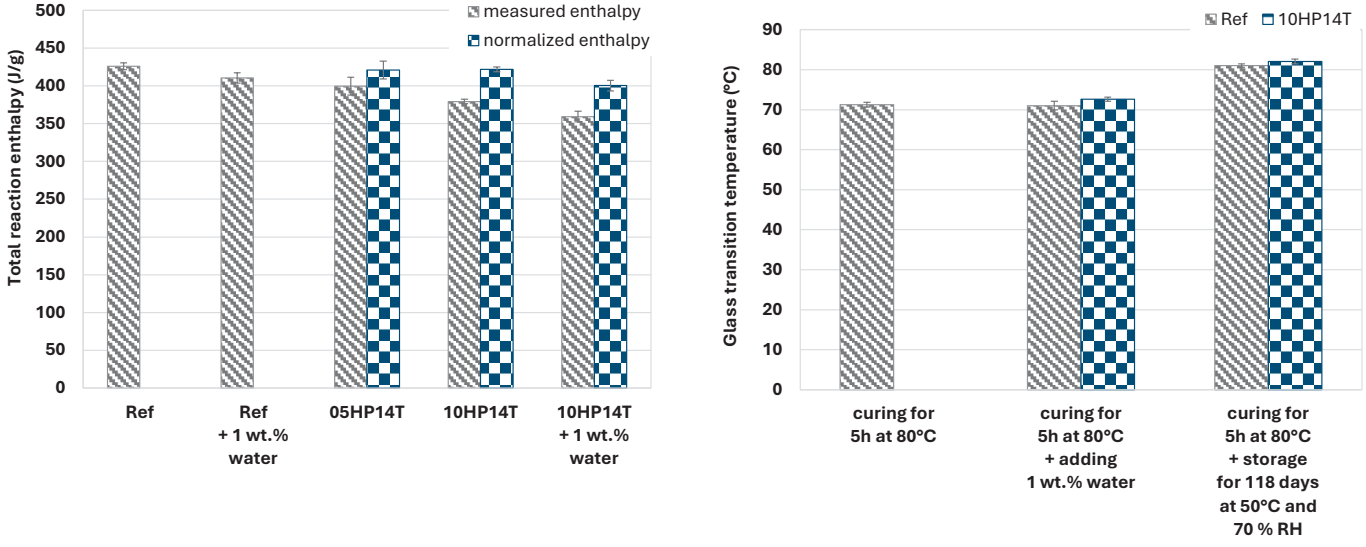

Fig. 11. Measured and normalized specific reaction enthalpies (left) and glass transition temperatures (right) of the epoxy resin as a function of nanoparticle fraction, water content and curing condition obtained by DSC. Conditions: Isothermal measurement at 80 °C for a duration of 300 min, content of HP14T nanoparticles: 5 and 10 wt%; epoxy resin: EPIKOTE RIMR 035c / EPIKURE RIMH 038.

enthalpy due to water could be attributed to the formation of micro-water phases and the isolation of hardener molecules by solvation. Furthermore, a reduction of functional groups, either through the conversion of the hardener's amine groups to non-reactive carbamates or the hydrolysis of epoxy groups within the resin, might also be discussed. The more pronounced influence of water on particle-modified systems is likely due to their lower resin content, resulting in a proportionally higher water mass relative to the resin and thus an increased impact.

The glass transition temperatures determined by DSC are presented on the right-hand side of Fig. 11. The results indicate that neither the addition of 1 wt% water nor the incorporation of 10 wt% boehmite particles has a significant influence on the glass transition temperature of the investigated resin system. In the unconditioned state, the resin systems exhibit glass transition temperatures in the range of 71–73 °C. No decrease in glass transition temperature attributable to hydrolysis was detected by DSC. In contrast, the saturated samples, which were stored for 118 days at 50 °C and 70 % relative humidity, posses glass transition temperatures approximately 10 K higher. This increase suggests that post-curing or additional crosslinking of the resin system occurred during exposure to hot and humid conditions.

4.3. Moisture absorption

The impact of moisture absorption on GFRP laminates, a critical environmental parameter, was investigated in this study. The analysis specifically addressed the effects of varying laminate thickness (1 to 3 fabric layers) and HP14T nanoparticle content (5 to 10 wt%). The samples are stored in a climate chamber at a temperature of 50 °C and a humidity of 70 %. After 115 days of storage a noticeable discoloration of the samples has taken place, see Fig. 12. This can be attributed to hygrothermal aging. While processes like matrix plasticization and swelling of fiber and matrix mainly affect the mechanical performance, chemical reactions like hydrolysis and oxidation of the epoxy can additionally lead to a change of color. The color changing to yellow–brown is characteristic for oxidation of epoxy resin and can even switch to a dark brown color at higher temperatures and longer exposure times [28].

Fig. 13 shows the saturation curves of the stored samples. All curves initially show an approximately Fickian behavior. Initially, the measurement curves increase linearly and flatten out significantly as saturation is approached. The maximum moisture absorption is approximately 0.25 wt% to 0.30 wt%. It is assumed that both parameters, the thickness of laminates varied by fabric layers and the content of nanoparticles, control the moisture absorption by different mechanisms. For the fiber layers acting the barrier effect is primarily discussed. In contrast, the effect of nanoparticles, due to their high specific surface, might be controlled by a combination of parameters: a) the hydrophilicity of the particle surface, which is determined by the chemical composition of the boehmite and the polar/ionic properties of taurine as a surface modifier; b) the formation of interphases, which cause altered local network densities and swelling properties; and c) the barrier effect of the nanoparticles, which lengthens the diffusion paths (tortuosity). These parameters have different effects on water absorption and maximum moisture saturation. Additionally, sample thickness significantly influences moisture absorption. Thinner samples exhibit steeper initial curves, indicating higher diffusion rates. This is further attributed to their larger specific surface area. Conversely, an increased number of fiber layers, and thus thicker samples, result in lower diffusion rates. This trend is explained by the barrier effect of the fiber layers, which hinder water molecule diffusion and consequently slow the diffusion process (tortuosity effect). Furthermore, thinner samples typically demonstrate a higher saturation moisture content. However, the saturation curves converge with prolonged storage time.

Nanoparticles further reduce the saturation moisture content of GFRPs, an effect consistently observed across all sample thicknesses for nanoparticle contents between 5 and 10 wt%. Specifically, a 5 wt% particle content reduces maximum moisture absorption by approximately 8–10 %. This suggests that the hindering and tortuosity effects of the particles are dominant, while the influence of the hydrophilic particle surface, which would typically increase moisture absorption, seems negligible. However, increasing the particle content to 10 wt% leads to an increase in moisture absorption. This counterintuitive trend is likely due to two factors: the larger proportion of hydrophilic particle surface contributing to increased water absorption, and the formation of an increased interphase with a morphology distinct from the bulk polymer. The lower network densities within these interphases might increase the free polymer volume, enabling local water incorporation (swelling effect). Moreover, macroscopic effects, such as the local introduction of pores during dispersion, must also be considered, as their increased frequency with higher particle content enables a higher degree of water absorption.

4.4. Tensile tests

Unidirectional specimens were used for the characterization of tensile properties. The modulus of elasticity (secant modulus), strength and strain to failure of saturated and dry specimens were determined perpendicular to the fiber orientation (matrix-dominated). The secant moduli were calculated for a given strain range between 0.05 and 0.25 %. The measurements were carried out as a function of filler content and temperature. The temperatures were selected on the basis of application limits based on DNVGL-ST-0376. Measurements were conducted at − 20 °C, 23 °C and 60 °C.

Fig. 14 shows the secant moduli determined. The secant modulus decreases with increasing temperature for all systems analyzed. The difference in the secant modulus at the test temperatures − 20 °C and 23 °C is very small. This can be explained by a large temperature difference to the measured glass transition temperature of approximately 80 °C. In the tests at 60 °C, the distance to the glass transition temperature is significantly smaller, resulting in a considerable decrease in the secant modulus. The increase in test temperature from − 20 °C to 23 °C leads to a reduction in the secant modulus of the unfilled reference system by approximately 8 %. An increase in temperature from − 20 °C to 60 °C, on the other hand, results in a decrease in the secant modulus of around 65 %. The particle-modified systems exhibit reductions in secant modulus of a similar magnitude due to an increased temperature.

Storage of the samples under hot-wet conditions leads to lower secant moduli for all material systems. The effect increases as the test

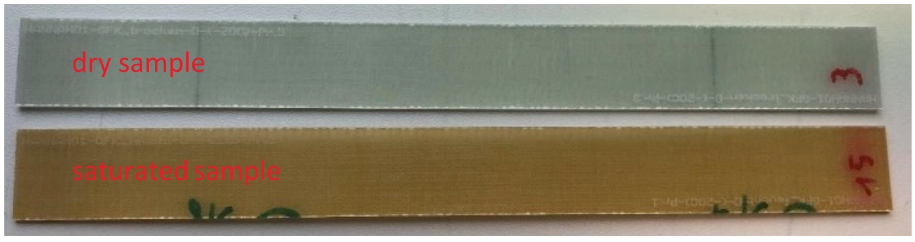

Fig. 12. Aging effect due to storage under hot-wet conditions (top: non-stored sample, bottom: sample stored for 115 days).

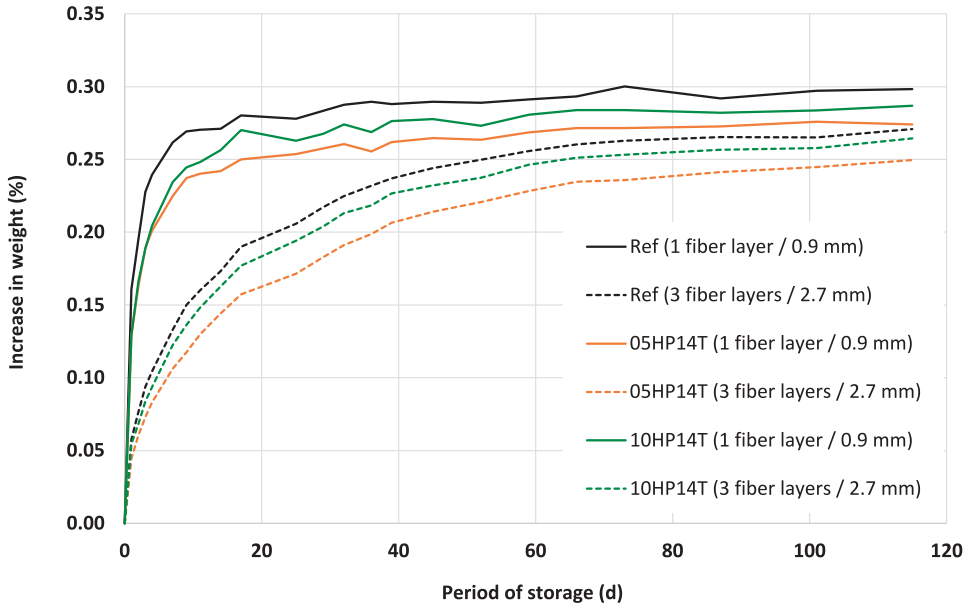

Fig. 13. Average moisture absorption of GFRP as a function of laminate thickness and nanoparticle content. Conditions: specimen dimensions: 50x50x0.9 mm for 1 fiber layer and 50x50x2.7 mm for 3 fiber layers; content of HP14T nanoparticles: 5 and 10 wt%; climate chamber: 50 °C and 70 % humidity. GFRP: FVC 53–55 %; UD (Saertex GF); epoxy resin: EPIKOTE RIMR 035c / EPIKURE RIMH 038.

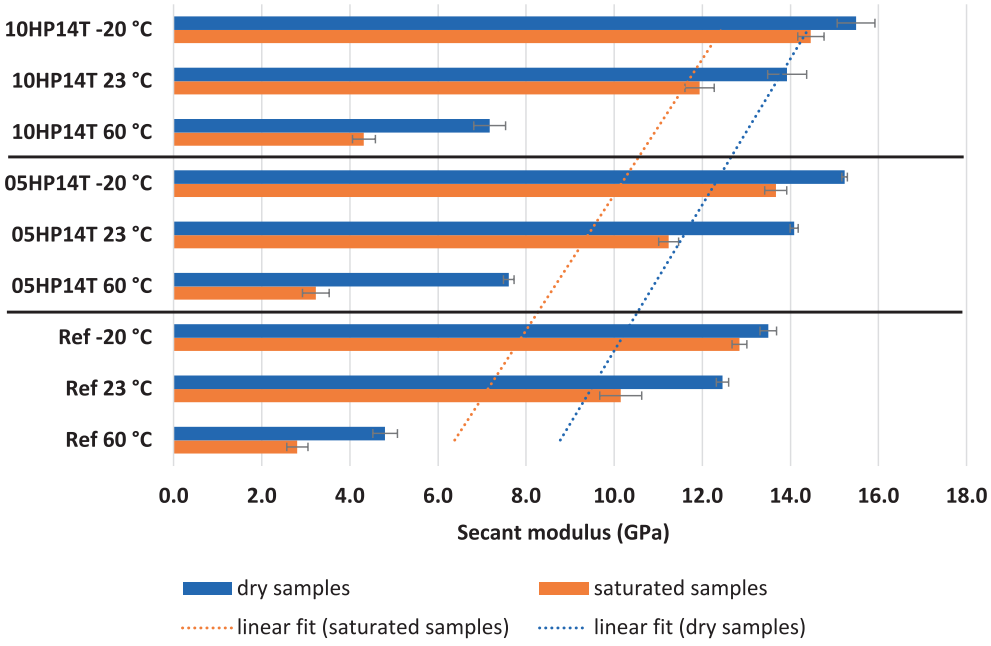

Fig. 14. Secant modulus of GFRP tested perpendicular to fiber orientation as a function of temperature, moisture and nanoparticle content. Conditions: temperature: −20 °C, 23 °C and 60 °C; dry samples stored at 23 °C and 50 % RH, saturated samples: stored under hot-wet conditions (60 °C, 85 % RH) until saturation; content of HP14T nanoparticles: 5 and 10 wt%; GFRP: [0°/0°], FVC 53–55 %; UD (Saertex GF); epoxy resin: EPIKOTE RIMR 035c / EPIKURE RIMH 038.

temperature rises. In the literature, this is associated with the occurrence of swelling stresses and a drop in the glass transition temperature due to water retention [2,6]. Furthermore, water absorption, especially at higher temperatures, can also lead to hydrolysis of the epoxy resin's chemical network, thereby causing softening effects. In this way, early plasticization also reduces stiffness. The fact that this effect is intensified with increasing test temperature is particularly evident in the example of the resin system with 5 wt% particles. At − 20 °C, the secant modulus is reduced by almost 1500 MPa. At 23 °C, the reduction increases to around 2800 MPa. A further increase in the test temperature to 60 °C results in a decrease in the secant modulus of 4400 MPa due to storage under hot-wet conditions, which corresponds to a percentage decrease in the secant modulus of almost 58 % compared to the dry sample.

By modifying the matrix with inorganic particles (boehmite), it can be assumed that the secant modulus increases, as the particles have a higher stiffness than the matrix. This behavior is also reflected in the results. For both the saturated and dry samples, the secant modulus increases with increasing particle content. The linear fits in Fig. 14 reveal that the increase in secant modulus due to the increasing particle content is approximately the same for dry and saturated samples.

Looking at the results for the ultimate tensile strengths, first of all, it should be mentioned that the strength of the unmodified epoxy system is

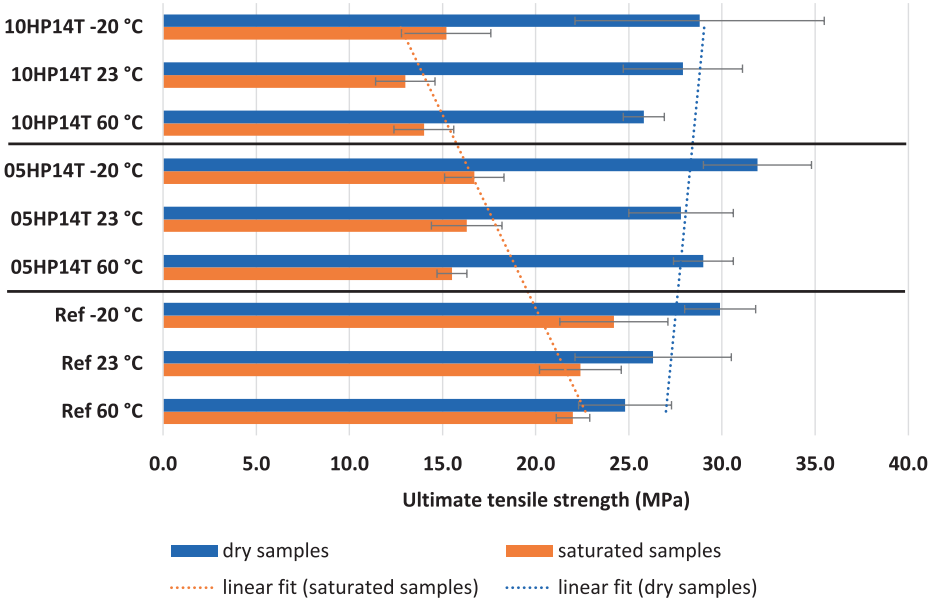

Fig. 15. Ultimate tensile strength of GFRP tested perpendicular to fiber orientation as a function of temperature, moisture and nanoparticle content. Conditions: temperature: −20 °C, 23 °C and 60 °C; dry samples stored at 23 °C and 50 % RH, saturated samples stored under hot-wet conditions (60 °C, 85 % RH) until saturation; content of HP14T nanoparticles: 5 and 10 wt%; GFRP: [0°/0°], FVC 53–55 %; UD (Saertex GF); epoxy resin: EPIKOTE RIMR 035c / EPIKURE RIMH 038.

70 N/mm^2 according to the manufacturer. The strengths determined in this work are significantly lower than the strength of the pure epoxy system. There are several possible explanations for this difference in strength. The fibers do not absorb any loads perpendicular to the fiber orientation. However, notch effects on the fibers can weaken the matrix. In addition, damage can occur at fiber crossing points (crossing of the fibers with the weft threads), which has a negative effect on the strength values as well. These effects are more pronounced with poor fiber–matrix adhesion. Fig. 16 clearly shows that the samples have a high number of weft threads. The lighter areas of the sample are areas where fiber–matrix debonding has occurred. These areas are particularly pronounced at the intersections of the fibers with the weft threads and along the weft threads.

The strengths of the tested 90° tensile specimens are plotted in Fig. 15. All epoxy systems tested show a tendency towards decreasing strength with increasing test temperature of up to 17 %. This effect is most pronounced in the dry samples. However, there is a large overlap in the standard deviations. The decreasing strengths can be explained by a softening of the matrix with increasing temperature.

The reduction in strengths due to moisture absorption is much more pronounced and ranges from 11 to 19 % for the reference samples. The loss of strength is again significantly increased by particle modification and reaches a maximum value of 53 % for the samples with 10 wt% HP14T.

The linear fits shown in Fig. 15 also illustrate that with increasing particle content the ultimate tensile strengths of the dry samples increase slightly by up to 2 % on average, whereas the strength of the saturated samples decreases significantly by up to 39 % on average. One explanation for the decreasing strength might be that absorbed water interacts with the fillers and causes particle–matrix debonding. These in turn lead to damage initiation under stress, resulting in premature failure and significantly reduced strength compared to the dry samples. This would also lead to a further reduction in strength with increasing particle content. Additional SEM images are required to validate the proposed mechanism.

The strains to failure determined for the test temperatures investigated are shown in Fig. 17. With increasing temperature, the strain to failure of the matrix should increase and thus also the strain to failure measured 90° to the fiber orientation. However, no clear trends can be recognized with regard to the influence of temperature due to similar average values and high standard deviations. One possible explanation is that the strain to failure is significantly influenced by the weft threads of the fiber layers. The weft threads consist of E-glass with 68 tex and make up approximately 3 % of the grammage of the fiber layers. If the strain to failure of E-glass is constant in the investigated temperature range, the temperature should also have no significant influence on the strain to failure of the GRP. Results produced by Ou and Zhu [22] support this explanation and show that the strain to failure of a GFRP with an epoxy resin matrix remains almost unchanged in the fiber direction in a temperature range from − 25 °C to 80 °C. The dry samples with 5 wt% HP14T at − 20 °C are an exception. For these samples, the strain to failure is higher compared to the other systems. The proportion of weft yarns is probably lower in these samples.

Storage under hot-wet conditions leads to a reduction in strain to failure of 7 to 11 % for the samples without particle modification. The addition of HP14T nanoparticles increases this effect, so that the strain to failure of the saturated samples is reduced by 47 to 62 % compared to the dry samples.

With regard to the influence of particles, it can be stated that the strain to failure of the dry samples remains almost constant with

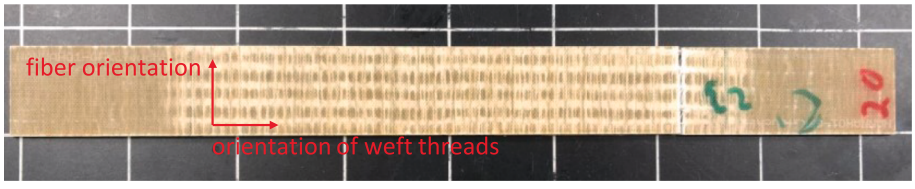

Fig. 16. 90°-tensile test specimen after completion of testing.

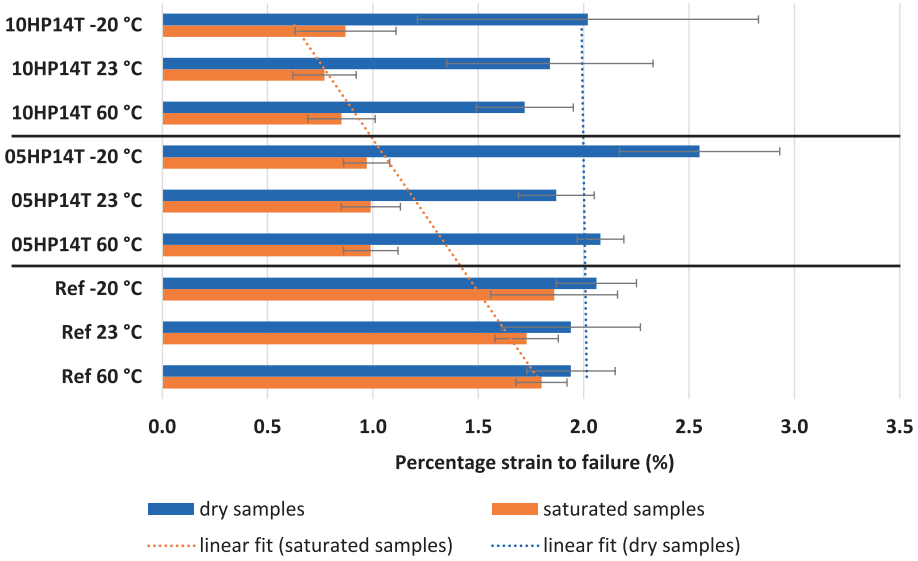

Fig. 17. Percentage strain to failure of GFRP tested perpendicular to fiber orientation as a function of temperature, moisture and nanoparticle content. Conditions: temperature: −20 °C, 23 °C and 60 °C; dry samples stored at 23 °C and 50 % RH, saturated samples stored under hot-wet conditions (60 °C, 85 % RH) until saturation; content of HP14T nanoparticles: 5 and 10 wt%; GFRP: [0°/0°], FVC 53–55 %; UD (Saertex GF); epoxy resin: EPIKOTE RIMR 035c / EPIKURE RIMH 038.

increasing particle content. In contrast, a clear trend can be recognized for the saturated samples. Here, an increase in particle content leads to a decrease in strain to failure. Compared to the unmodified epoxy system, the addition of 5 wt% HP14T leads to a reduction in strain to failure of 43–48 % at the test temperatures analyzed. Increasing the particle content to 10 wt% increases this effect to 53–56 %. In this context, it can also be argued that absorbed water favors the debonding of particles and matrix, which can lead to damage initialization under load. This in turn leads to premature failure and a decrease in strain to failure with increasing particle content.

For all tensile tests performed, the scattering of the test results may be attributed to the weft threads of the E-glass fabric. The weft threads are to a large extend not aligned uniformly throughout the fabric, referring to distances between weft threads and the angle between glass fiber rovings and weft threads. Thus, fraction and alignment of the weft threads may vary from sample to sample leading to an increased scattering.

5. Summary and conclusion

First, the influence of temperature and particle content on the rheological properties of the epoxy resin system was investigated. As the temperature increases, the speed of viscosity build up is significantly accelerated, but the initial viscosity also decreases. The pot life was increased due to the lower initial viscosity. The addition of HP14T nanoparticles leads to an increase in the initial viscosity and to a slight increase in viscosity build up. These effects increase with increasing particle content. However, the influence of the temperature is significantly stronger than the influence of the HP14T nanoparticles. When manufacturing the test panels, the negative effect of the particles on the viscosity can be compensated by increasing the temperature and applying shear stress.

The influence of moisture and particle content on network formation was also investigated using DSC measurements. Both the addition of water and HP14T nanoparticles seem to reduce the measured reaction enthalpy. However, if the samples are normalized to the content of the resin system, there is only a slight decrease in the reaction enthalpy due to increasing particle content (steric hindrance). The decrease in enthalpy due to water can be attributed to the formation of micro-water phases and the isolation of hardener molecules (solvation).

To determine the moisture absorption, samples were stored under hot-wet conditions. The samples stored varied in terms of the number of fiber layers and the level of particle content. The recorded saturation curves show an approximately Fickian behavior with an initial linear moisture absorption, which then flattens out and changes to a saturation state. Different mechanisms are suggested for the observed results. Samples with a lower number of fiber layers (barrier layers) reach the saturation state significantly earlier. With a low particle content, moisture absorption is also slowed down by the particles (tortuosity effect). By increasing the particle content, the moisture absorption approaches the GRP without particles again, which is mainly attributed to the hydrophilic character of the particles.

The influence of moisture and particle content on the mechanical properties was investigated using tensile tests at different test temperatures. The results show that at all test temperatures, the secant modulus, ultimate tensile strength and strain to failure decrease due to storage under hot-wet conditions. This effect is intensified by HP14T nanoparticles. The influence of temperature is also observed. Secant modulus and ultimate tensile strength decrease slightly with increasing temperature. The closer the test temperature to the samples' glass transition temperature, the stronger the influence of temperature. The secant modulus increases slightly with increasing particle content for both dry and saturated samples. Ultimate tensile strength and strain to failure increase slightly or remain almost constant with increasing particle content for the dry samples, but decrease for the saturated samples with increasing particle content.

In summary, this study reveals that nanoparticle content, temperature and moisture significantly influence the thermal and mechanical properties of a wind-turbine-proven epoxy resin and the corresponding GFRP, see Table 4. While a higher nanoparticle content (10 wt%) enhances material properties, it simultaneously compromises processing characteristics by reducing the pot life and increasing initial viscosity. Optimizing the nanoparticle content by balancing processing and material-related parameters is the key to exploit the full potential of the investigated material. Furthermore, developing a fundamental understanding of the hygrothermal aging mechanism and additional fatigue testing of the nanoparticle-modified GFRP are essential to provide a holistic evaluation of the material performance.

CRediT authorship contribution statement

Maximilian Jux: Writing – original draft, Visualization, Validation,

Table 4
Overview of measured properties. Content of HP14T nanoparticles: 5 and 10 wt.%; GFRP: [90/90], FVC 53–55 %; UD (Saertex GF); epoxy resin: EPIKOTE RIMR 035c / EPIKURE RIMH 038.

Resin system	Rheological properties - isotherm (samples without fibers)				Enthalpy (samples without fibers)		Max. moisture absorption (glass fiber reinforced samples)		90°-tensile properties[a] (glass fiber reinforced samples)					
	T[b] (°C)	Initial viscosity (Pas)	Time to reach 0.5 Pas (min)	Time to reach 100 Pas (min)	Samples without water (J/g)	Samples with 1 wt.% water (J/g)	1-layer GFRP (%)	3-layers GFRP (%)	T[b] (°C)	Secant modulus (GPa) Dry	Secant modulus (GPa) Hot-wet	Ultimate tensile strength (MPa) Dry	Ultimate tensile strength (MPa) Hot-wet	Percentage strain to failure (%) Dry	Percentage strain to failure (%) Hot-wet
Unmodified reference	23	0.359±0.013	64.4±14.1	578.0±2.8	426.0±4.5	410.7±6.8	0.298 ±0.010	0.271 ±0.005	-20	13.5±0.2		29.9±1.9			
	40	0.112±0.014	98.3±6.9	265.6±6.6					23	12.8±0.2		24.2±2.2		2.1±0.2	1.9±0.3
	50	0.060±0.003	74.2±2.6	163.6±4.1					60	12.5±0.1		26.3±4.2		1.9±0.3	1.7±0.2
										10.1±0.5		22.4±2.2		1.9±0.2	1.8±0.1
										4.8±0.3	2.8±0.2	24.8±2.5			
												22.0±0.9			
Modified with 5 wt.% boehmite (HP14T)	23	0.681±0.047	-	553.1±4.1	399.9±11.9	-	0.274 ±0.008	0.250 ±0.005	-20	15.2±0.1		31.9±2.9			
	40	0.253±0.007	59.2±0.6	242.0±1.1	421.2±11.9[c]				23	13.7±0.3		16.7±1.6		2.6±0.4	1.0±0.1
									60	14.1±0.1		27.8±2.8		1.9±0.2	1.0±0.1
										11.2±0.2		16.3±1.9		2.1±0.1	1.0±0.1
										7.6±0.1	3.2±0.3	29.0±1.6			
												15.5±0.8			
Modified with 10 wt.% boehmite (HP14T)	23	1.380±0.082	10.7±0.0	454.0±8.3	379.4±3.1	359.4±7.1	0.287 ±0.014	0.264 ±0.008	-20	15.5±0.4		28.8±6.7			
	40	0.617±0.076	22.5±1.2	205.7±1.9	422.0±3.1[c]	400.5±7.1[c]			23	14.5±0.3		15.2±2.4		2.0±0.8	0.9±0.2
	50	0.451±0.023		119.7±2.6					60	13.9±0.4		27.9±3.2		1.8±0.5	0.8±0.2
										11.9±0.3		13.0±1.6		1.7±0.2	0.9±0.2
										7.2±0.4	4.3±0.3	25.8±1.1			
												14.0±1.6			

[a] Tensile tests were performed with GFRP samples [0°/0°] with tensile load at 90° to the fiber orientation (matrix dominated). Dry—samples stored at 23 °C and 50% RH, hot-wet—samples stored under hot-wet conditions (60 °C, 85% RH) until saturation.
[b] Rheological and tensile properties were determined at different temperatures.
[c] Normalized enthalpy, referenced to the resin content of the sample.

Methodology, Investigation, Conceptualization. **Thorsten Mahrholz:** Writing – review & editing, Writing – original draft, Methodology, Conceptualization. **Peter Wierach:** Writing – review & editing, Supervision, Project administration, Funding acquisition.

Declaration of competing interest

The authors declare that they have no known competing financial interests or personal relationships that could have appeared to influence the work reported in this paper.

Acknowledgement

The work presented in this paper was funded by the Federal Ministry of Economics and Energy within the framework of the HANNAH joint project, titled “Challenges of the industrial application of nanomodified and hybrid material systems in lightweight rotor blade construction” (grant number 0324345B). The authors thank the project partners from the Leibniz University (Institute of Structural Analysis), the Fraunhofer Society (Institute for Wind Energy Systems (IWES), and the industrial partners INVENT and Zeisberg-Carbon for their valuable discussions and for providing us with samples and material data. Special thanks are also due to Professor R. Rolfes, Head of the Institute of Structural Analysis, for successfully supporting and coordinating this and other joint projects in the past. This contribution is dedicated to him on the occasion of his 65th birthday.

References

[1] Hau E. Windkraftanlagen. fifth ed. Berlin Heidelberg: Springer; 2014.
[2] M. Li, TEMPERATURE AND MOISTURE EFFECTS ON COMPOSITE MATERIALS FOR WIND TURBINE BLADES, Master’s Thesis, MONTANA STATE UNIVERSITY, 2000.
[3] Gupta AK, Kiran R, Zafar S, Pathak H. Effect of hygrothermal ageing on the mechanical properties of glass fiber reinforced polymer composite: experimental and numerical approaches. Mater TodayCommunications 2024;41:1–12. https://doi.org/10.1016/j.mtcomm.2024.111060.
[4] Civil Engineering Portal, Impingement Of Environmental Factors That Defines A System On Composites Performance, https://www.engineeringcivil.com/impingement-of-environmental-factors-that-defines-a-system-on-composites-performance.html, 2013 (accessed 28 July 2025).
[5] Abdel-Magid B, Ziaee S, Gass K, Schneider M. The combined effects of load, moisture and temperature on the properties of E-glass/epoxy composites. Compos Struct 2005;71:320–6. https://doi.org/10.1016/j.compstruct.2005.09.022.
[6] Marom G. Environmental effects on fracture mechanical properties of polymer composites. In: Friedrich K, editor. Composite Materials Series, 6. Elsevier; 1989. p. 397–424.
[7] Paschen H, Coenen C, Fleischer T, Grünwald R, Oertel D, Revermann C. Nanotechnologie. first ed. Berlin Heidelberg: Springer; 2004.
[8] Chen L, He X, Liu H, Qian L, Kim SH. Water adsorption on hydrophilic and hydrophobic surfaces of silicon. J Phys Chem C 2018;122:11385–91. https://doi.org/10.1021/acs.jpcc.8b01821.
[9] Liu W, Hoa SV, Pugh M. Water uptake of epoxy-clay nanocomposites: experiments and model validation. Compos Sci Technol 2008;68:2066–72. https://doi.org/10.1016/j.compscitech.2007.07.024.
[10] Chow WS. Water absorption of epoxy/glass fiber/organo-montmorillonite nanocomposites. Express Polym Lett 2007;1:104–8. https://doi.org/10.3144/expresspolymlett.2007.18.
[11] Becker O, Varley RJ, Simon GP. Thermal stability and water uptake of high performance epoxy layered silicate nanocomposites. Eur Polym J 2004;40:187–95. https://doi.org/10.1016/j.eurpolymj.2003.09.008.
[12] Nomai J. On the effect of nanofillers on the environmental stress cracking resistance of glassy polymers, dissertation. Technische Universität Kaiserslautern 2019.
[13] Gatos KG, Martínez Alcázar JG, Psarras GC, Thomann R, Karger-Kocsis J. Polyurethane latex/water dispersible boehmite alumina nanocomposites: thermal, mechanical and dielectrical properties. Compos Sci Technol 2007;67:157–67. https://doi.org/10.1016/j.compscitech.2006.07.025.
[14] Chin JW, Nguyen T, Aouadi K. Sorption and diffusion of water, salt water, and concrete pore solution in composite matrices. J Appl Polym Sci 1999;71:483–92. https://doi.org/10.1002/(SICI)1097-4628(19990118)71:3<483::AID-APP15>3.0.CO;2-S.
[15] C.L. Soles, F.T. Chang, B.A. Bolan, H.A. Hristov, D.W. Gidley, A.F. Yee, Contributions of the nanovoid structure to the moisture absorption properties of epoxy resins, J. Polym. Sci., Part B: Polym. Phys. 36 (1998) 3035 – 3048, https://doi.org/10.1002/(SICI)1099-0488(199812)36:17<3035::AID-POLB4>3.0.CO;2-Y.
[16] Schutte CL. Environmental durability of glass-fiber composites. Mater Sci Eng R 1994;13:265–323. https://doi.org/10.1016/0927-796X(94)90002-7.
[17] Vaddadi P, Nakamura T, Singh RP. Inverse analysis for transient moisture diffusion through fiber-reinforced composites. Acta Mater 2003;51:177–93. https://doi.org/10.1016/S1359-6454(02)00390-7.
[18] Grant TS, Bradley WL. In-situ observations in SEM of degradation of graphite/epoxy composite materials due to seawater immersion. J Compos Mater 1995;29:852–67. https://doi.org/10.1177/002199839502900701.
[19] Lundgren JE, Gudmundson P. A model for moisture absorption in cross-ply composite laminates with matrix cracks. J Compos Mater 1998;32:2226–53. https://doi.org/10.1177/002199839803202403.
[20] Jia Z, Li T, Chiang F, Wang L. An experimental investigation of the temperature effect on the mechanics of carbon fiber reinforced polymer composites. Compos Sci Technol 2018;154:53–63. https://doi.org/10.1016/j.compscitech.2017.11.015.
[21] Jux M, Sinapius M. Effect of particle-surface-modification on the failure behavior of epoxy/boehmite CFRPs. In: Sinapius M, Ziegmann G, editors. Acting Principles

of Nano-Scaled Matrix Additives for Composite Structures. Switzerland: Springer; 2021. p. 411–31.
[22] Jux M, Fankhänel J, Daum B, Mahrholz T, Sinapius M, Rolfes R. Mechanical properties of epoxy/boehmite nanocomposites in dependency of mass fraction and surface modification - an experimental and numerical approach. Polymer 2018; 141:34–45. https://doi.org/10.1016/j.polymer.2018.02.059.
[23] Jux M, Finke B, Mahrholz T, Sinapius M, Kwade A, Schilde C. Effects of Al(OH)O nanoparticle agglomerate size in epoxy resin on tension, bending, and fracture properties. J Nanopart Res 2017;19:1–13. https://doi.org/10.1007/s11051-017-3831-9.
[24] Exner W, Arlt C, Mahrholz T, Riedel U, Sinapius M. Nanoparticles with various surface modifications as functionalized cross-linking agents for composite resin materials. Compos Sci Technol 2012;72:1153–9. https://doi.org/10.1016/j.compscitech.2012.03.024.
[25] Adam TJ, Exner W, Wierach P. Taurine-modified boehmite nanoparticles for GFRP wind turbine rotor blade fatigue life enhancement. Materials 2021;14:1–21. https://doi.org/10.3390/ma14226997.
[26] Memon NA. Rheology of polycarbonate/poly(butylene terephthalate) blends containing a core-shell modifier and high-molecular-weight acrylic polymers: extrusion blow-moldable resins. J Appl Polym Sci 1994;54:1059–72. https://doi.org/10.1002/app.1994.070540808.
[27] Hoebbel D, Nacken M, Schmid H. The effect of nanoscaled metal oxide sols on the structure and properties of glycidoxypropyltrimethoxysilane derived sols and gels. J Sol-Gel Sci Technol 2000;19:305–9. https://doi.org/10.1023/A:1008777414416.
[28] Zhang Y, Wan H, Li B. Study on the thermal-oxidative aging performance of glass fiber reinforced epoxy composites. Polymer 2025;334:1–12. https://doi.org/10.1016/j.polymer.2025.128707.